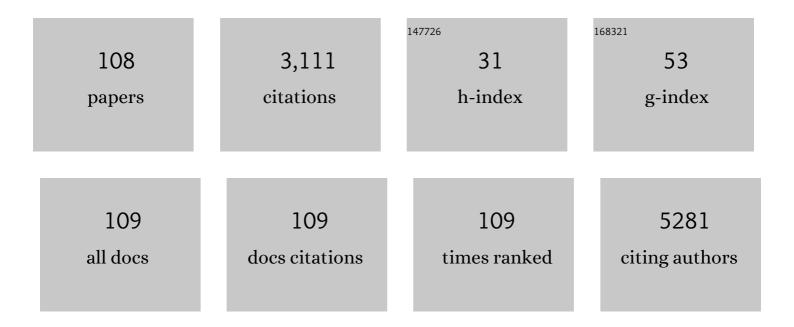
List of Publications by Year in descending order

Source: https://exaly.com/author-pdf/2965734/publications.pdf Version: 2024-02-01



#	Article	IF	CITATIONS
1	Investigation into the Interaction between Surface-Bound Alkylamines and Gold Nanoparticles. Langmuir, 2003, 19, 6277-6282.	1.6	469
2	Phase transfer of silver nanoparticles from aqueous to organic solutions using fatty amine molecules. Journal of Colloid and Interface Science, 2003, 264, 396-401.	5.0	156
3	Photocatalytic degradation of methylene blue with Cu doped ZnS nanoparticles. Journal of Luminescence, 2014, 145, 6-12.	1.5	128
4	Formation of Water-Dispersible Gold Nanoparticles Using a Technique Based on Surface-Bound Interdigitated Bilayers. Langmuir, 2003, 19, 1168-1172.	1.6	124
5	Structural and optical study of Li doped CuO thin films on Si (100) substrate deposited by pulsed laser deposition. Applied Surface Science, 2014, 307, 280-286.	3.1	105
6	Structural and photocatalytic studies of Mn doped TiO2 nanoparticles. Spectrochimica Acta - Part A: Molecular and Biomolecular Spectroscopy, 2012, 98, 256-264.	2.0	91
7	Gold Nanoparticles Assembled on Amine-Functionalized Naâ^'Y Zeolite:Â A Biocompatible Surface for Enzyme Immobilization. Langmuir, 2003, 19, 3858-3863.	1.6	90
8	DNA-mediated electrostatic assembly of gold nanoparticles into linear arrays by a simple drop-coating procedure. Applied Physics Letters, 2001, 78, 2943-2945.	1.5	81
9	Highly Oriented Gold Nanoribbons by the Reduction of Aqueous Chloroaurate lons by Hexadecylaniline Langmuir Monolayers. Chemistry of Materials, 2003, 15, 17-19.	3.2	79
10	Sequential Electrostatic Assembly of Amine-Derivatized Gold and Carboxylic Acid-Derivatized Silver Colloidal Particles on Glass Substrates. Langmuir, 2000, 16, 6921-6926.	1.6	76
11	Structural and optical properties of ZnO nanoparticles synthesized at different pH values. Journal of Alloys and Compounds, 2012, 539, 174-178.	2.8	69
12	Structural, optical and ferroelectric behavior of CuO nanostructures synthesized at different pH values. Superlattices and Microstructures, 2013, 60, 129-138.	1.4	67
13	Visible-light photocatalytic degradation of methylene blue with Fe doped CdS nanoparticles. Applied Surface Science, 2013, 270, 655-660.	3.1	66
14	Photocatalytic degradation of methylene blue with Fe doped ZnS nanoparticles. Spectrochimica Acta - Part A: Molecular and Biomolecular Spectroscopy, 2013, 113, 250-256.	2.0	65
15	Amphoterization of Colloidal Gold Particles by Capping with Valine Molecules and Their Phase Transfer from Water to Toluene by Electrostatic Coordination with Fatty Amine Molecules. Langmuir, 2000, 16, 9775-9783.	1.6	64
16	Effect of NaOH molar concentration on morphology, optical and ferroelectric properties of hydrothermally grown CuO nanoplates. Materials Science in Semiconductor Processing, 2015, 38, 72-80.	1.9	57
17	Growth of Calcium Carbonate Crystals within Fatty Acid Bilayer Stacks. Langmuir, 2002, 18, 6075-6080.	1.6	56
18	Photocatalytic studies of silver doped ZnO nanoparticles synthesized by chemical precipitation method. Journal of Sol-Gel Science and Technology, 2012, 63, 546-553.	1.1	55

#	Article	IF	CITATIONS
19	Structural and optical characterization of Zn doped TiO2 nanoparticles prepared by sol–gel method. Journal of Sol-Gel Science and Technology, 2012, 61, 585-591.	1.1	52
20	Fragmentation cross sections of Fe26+, Si14+ and C6+ ions of 0.3–10 on polyethylene, CR39 and aluminum targets. Nuclear Physics A, 2008, 807, 206-213.	0.6	50
21	Structural, morphological and optical study of Li doped ZnO thin films on Si (100) substrate deposited by pulsed laser deposition. Ceramics International, 2014, 40, 11915-11923.	2.3	48
22	Synthesis of Ag/Pd Nanoparticles and Their Low-Temperature Alloying within Thermally Evaporated Fatty Acid Films. Journal of Physical Chemistry B, 2002, 106, 297-302.	1.2	47
23	Phase Transfer of Aqueous CdS Nanoparticles by Coordination with Octadecanethiol Molecules Present in Nonpolar Organic Solvents. Langmuir, 2000, 16, 9299-9302.	1.6	44
24	Magnetic monopole search at high altitude with the SLIM experiment. European Physical Journal C, 2008, 55, 57-63.	1.4	44
25	Morphology of BaSO4 Crystals Grown on Templates of Varying Dimensionality:  The Case of Cysteine-Capped Gold Nanoparticles (0-D), DNA (1-D), and Lipid Bilayer Stacks (2-D). Crystal Growth and Design, 2002, 2, 197-203.	1.4	37
26	Results of the search for strange quark matter and Q-balls withÂthe SLIM experiment. European Physical Journal C, 2008, 57, 525-533.	1.4	37
27	Effect of NaOH molar concentration on optical and ferroelectric properties of ZnO nanostructures. Applied Surface Science, 2015, 356, 438-446.	3.1	37
28	Structural, optical and ferroelectric behavior of hydrothermally grown ZnO nanostructures. Superlattices and Microstructures, 2013, 64, 331-342.	1.4	36
29	Variation in morphology of gold nanoparticles synthesized by the spontaneous reduction of aqueous chloroaurate ions by alkylated tyrosine at a liquid–liquid and air–water interface. Journal of Materials Chemistry, 2004, 14, 2696.	6.7	35
30	Phase transfer of platinum nanoparticles from aqueous to organic solutions using fatty amine molecules. Journal of Chemical Sciences, 2004, 116, 293-300.	0.7	34
31	Energy storage properties of double perovskites Gd2NiMnO6 for electrochemical supercapacitor application. Solid State Sciences, 2020, 105, 106252.	1.5	34
32	Acoustic emission characteristics and b-value estimate in relation to waveform analysis for damage response of snow. Cold Regions Science and Technology, 2015, 119, 170-182.	1.6	33
33	Growth of thermally evaporated SnO2 nanostructures for optical and humidity sensing application. Sensors and Actuators B: Chemical, 2014, 201, 369-377.	4.0	31
34	Moon and Sun shadowing effect in the MACRO detector. Astroparticle Physics, 2003, 20, 145-156.	1.9	29
35	Enhanced photocatalytic performance of m-WO3 and m-Fe-doped WO3 cuboids synthesized via sol-gel approach using egg albumen as a solvent. Materials Science in Semiconductor Processing, 2019, 104, 104690.	1.9	29
36	Synthesis, structural and photocatalytic studies of Mn-doped CdS nanoparticles. Research on Chemical Intermediates, 2013, 39, 645-657.	1.3	25

#	Article	IF	CITATIONS
37	Structural, optical, and ferroelectric behavior of Zn1â^'xLixO (0⩽x⩽0.09) nanostructures. Journal of Alloys and Compounds, 2014, 585, 345-351.	2.8	23
38	MoS ₂ nanoparticle/activated carbon composite as a dual-band material for absorbing microwaves. Nanoscale Advances, 2021, 3, 4196-4206.	2.2	22
39	Low temperature crystalline Ag–Ni alloy formation from silver and nickel nanoparticles entrapped in a fatty acid composite film. Applied Physics Letters, 2001, 79, 3314-3316.	1.5	21
40	Structural and optical characterization of Ag-doped TiO2 nanoparticles prepared by a sol–gel method. Research on Chemical Intermediates, 2012, 38, 1443-1453.	1.3	18
41	Excellent microwave absorbing and electromagnetic shielding performance of grown MWCNT on activated carbon bifunctional composite. Carbon, 2022, 198, 151-161.	5.4	18
42	Structures and optical properties of Zn1â^'x Ni x O nanoparticles by coprecipitation method. Research on Chemical Intermediates, 2012, 38, 1483-1493.	1.3	17
43	Activated carbon derived from mango leaves as an enhanced microwave absorbing material. Sustainable Materials and Technologies, 2021, 27, e00244.	1.7	17
44	Structural, optical and photocatalytic studies of Fe doped ZnS nanoparticles. Journal of Sol-Gel Science and Technology, 2013, 67, 376-383.	1.1	16
45	Search for intermediate mass magnetic monopoles and nuclearites with the SLIM experiment. Radiation Measurements, 2005, 40, 405-409.	0.7	15
46	The dielectric behavior of Zn1â^'xNixO/NiO two-phase composites. Journal Physics D: Applied Physics, 2014, 47, 435305.	1.3	15
47	Engineered perovskite LaCoO3/rGO nanocomposites for asymmetrical electrochemical supercapacitor application. Journal of Materials Science: Materials in Electronics, 2022, 33, 2590-2606.	1.1	14
48	Calibration of the Makrofol–DE nuclear track detector using relativistic lead ions. Radiation Measurements, 2005, 40, 433-436.	0.7	13
49	Influence of silver and graphite on zinc oxide nanostructures for optical application. Optical Materials, 2013, 35, 1335-1341.	1.7	13
50	Experimental measurements of acoustical properties of snow and inverse characterization of its geometrical parameters. Applied Acoustics, 2016, 101, 15-23.	1.7	13
51	Enhanced microwave absorption properties of Co and Ni co-doped iron (II,III)/reduced graphene oxide composites at X-band frequency. Journal of Materials Science: Materials in Electronics, 2019, 30, 19325-19334.	1.1	13
52	Study of optical And Ferroelectric Behavior Of ZnO Nanostructures. Advanced Materials Letters, 2013, 4, 220-224.	0.3	13
53	Water-dispersible nanoparticles via interdigitation of sodium dodecylsulphate molecules in octadecylamine-capped gold nanoparticles at a liquid-liquid interface. Journal of Chemical Sciences, 2003, 115, 679-687.	0.7	12
54	Multi-sensor couplers and waveguides for efficient detection of acoustic emission behavior of snow. Cold Regions Science and Technology, 2014, 101, 1-13.	1.6	12

#	Article	IF	CITATIONS
55	Synthesis of N and F co-doped TiO2 nanophotocatalysts for degradation of malathion in water. Research on Chemical Intermediates, 2017, 43, 387-399.	1.3	12
56	Study of photoluminescence and nonlinear optical behaviour of AgCu nanoparticles for nanophotonics. Nano Structures Nano Objects, 2021, 28, 100807.	1.9	11
57	Organoamine Templated Multifunctional Hybrid Metal Phosphonate Frameworks: Promising Candidates for Tailoring Electrochemical Behaviors and Size-Selective Efficient Heterogeneous Lewis Acid Catalysis. Inorganic Chemistry, 2022, 61, 9580-9594.	1.9	11
58	Nickel-induced structural, optical, magnetic, and electrical behavior of α-Fe ₂ O ₃ . Physica Status Solidi (B): Basic Research, 2014, 251, 1552-1557.	0.7	10
59	Facile synthesis of bulk SnO 2 and ZnO tetrapod based graphene nanocomposites for optical and sensing application. Materials Chemistry and Physics, 2017, 201, 372-383.	2.0	10
60	Microstructural evolution and photoluminescence performanance of nickel and chromium doped ZnO nanostructures. Materials Chemistry and Physics, 2018, 205, 9-15.	2.0	10
61	Novel green photo-catalyst â€~turmeric roots' for pesticides degradation: Preparation and characterizations. Materials Letters, 2020, 262, 127030.	1.3	10
62	Effect of Nanographite on Electrical Mechanical and Wear Characteristics of Graphite Epoxy Composites. Defence Science Journal, 2020, 70, 306-312.	0.5	10
63	Formation of platinum nanoparticles at air–water interfaces by the spontaneous reduction of subphase chloroplatinate anions by hexadecylaniline Langmuir monolayers. Journal of Colloid and Interface Science, 2004, 271, 381-387.	5.0	9
64	Biogenesis of PbS Nanocrystals by Using Rhizosphere Fungus i.e., Aspergillus sp. Isolated from the Rhizosphere of Chickpea. BioNanoScience, 2014, 4, 189-194.	1.5	9
65	Structural, Optical, and Ferroelectric Behaviors of Cu1â^'x Li x O (0Ââ‰ÂxÂâ‰Â0.09) Nanostructures. Acta Metallurgica Sinica (English Letters), 2014, 27, 306-312.	1.5	9
66	Multifunctional silanized silica nanoparticle functionalized graphene oxide: polyetherimide composite film for EMI shielding applications. Journal of Materials Science: Materials in Electronics, 2018, 29, 14122-14131.	1.1	8
67	Trace uranium analysis of water from the south-west coastal region of India. Journal of Radioanalytical and Nuclear Chemistry, 1994, 178, 245-251.	0.7	7
68	Crystallization of SrCO3 within thermally evaporated fatty acid films: unusual morphology of crystal aggregates. CrystEngComm, 2001, 3, 81.	1.3	7
69	Study of CuO Nanoparticles Synthesized by Sol-gel Method. AIP Conference Proceedings, 2011, , .	0.3	7
70	Fragmentation cross-section of 600 A MeV Si14+ ions in thick polyethylene target. European Physical Journal A, 2013, 49, 1.	1.0	7
71	Biomass-Derived Activated Carbon/Epoxy Composite as Microwave Absorbing Material. Journal of Electronic Materials, 2022, 51, 2918-2925.	1.0	7
72	Lamellar multilayer hexadecylaniline-modified gold nanoparticle films deposited by the Langmuir-Blodgett technique. Journal of Chemical Sciences, 2003, 115, 185-193.	0.7	6

#	Article	IF	CITATIONS
73	Calibration of CR39 detectors with new system for Fe26+ ion beam and measurement of total charge changing cross-section in Al target. Radiation Measurements, 2012, 47, 1023-1029.	0.7	6
74	Validation of Geant4 physics models for 56Fe ion beam in various media. Nuclear Instruments & Methods in Physics Research B, 2012, 291, 7-11.	0.6	6
75	Simulation of depth–dose distributions for various ions in polyethylene medium. Advances in Space Research, 2012, 49, 1691-1697.	1.2	6
76	Phase transformation in wet chemically synthesized Y2NiFeO6, and its magnetic and energy storage properties. Applied Physics A: Materials Science and Processing, 2020, 126, 1.	1.1	6
77	Structural, Dielectric, and Energy Storage Properties of Citric Acid and Ethylene Glycol Assisted Hydrothermally Synthesized Y ₂ FeCoO ₆ . Physica Status Solidi (A) Applications and Materials Science, 2020, 217, 2000324.	0.8	6
78	Excellent microwave absorbing performance of biomass-derived activated carbon decorated with <i>in situ</i> -grown CoFe ₂ O ₄ nanoparticles. Materials Advances, 2022, 3, 2533-2545.	2.6	6
79	Microanalysis of uranium in Antarctica soil samples using fission track method. Journal of Radioanalytical and Nuclear Chemistry, 1995, 191, 381-386.	0.7	5
80	Modification in mechanical, tribological & electrical properties of epoxy at low weight fraction of multiwalled carbon nanotube. Materials Today: Proceedings, 2020, 26, 1836-1840.	0.9	5
81	Morphology of BaSO4 crystals grown at the liquid?liquid interface. CrystEngComm, 2001, 3, 213.	1.3	4
82	First results of the CAKE experiment. Radiation Measurements, 2003, 36, 335-338.	0.7	4
83	Anion intercalation pseudo-capacitance performance of oxygen-deficient double perovskite prepared via facile wet chemical route. Materials Science in Semiconductor Processing, 2022, 138, 106300.	1.9	4
84	Analog ensembleÂ(AE) systems for real time quantitative precipitation forecasts (QPFs) for different forecast lead times at local scale over the north-westÂHimalaya (NWH), India. Meteorology and Atmospheric Physics, 2021, 133, 533-552.	0.9	3
85	Effect of calcinations on structural, optical and photocatalytic properties of a green photo-catalyst †turmeric roots powder'. Optik, 2020, 216, 164804.	1.4	3
86	Effect of In additive on the photosensitivity of glassy Se80Te20alloy. Journal of Modern Optics, 2009, 56, 1272-1275.	0.6	2
87	Response of CR39 detector to 5A GeV Si14+ ions and measurement of total charge changing cross-section. Radiation Physics and Chemistry, 2013, 92, 8-13.	1.4	2
88	Impedance modeling for classification of flavored green teas. Turkish Journal of Electrical Engineering and Computer Sciences, 2015, 23, 2208-2214.	0.9	2
89	The impacts of the approaching western disturbances (WDs) on the surface meteorological variables over the north-west Himalaya (NWH), India. Journal of Earth System Science, 2019, 128, 1.	0.6	2
90	Symmetric/asymmetric energy storage device of reduced graphene oxide assisted LaNi0.9Co0.1O3 perovskite nanomaterials. Applied Physics A: Materials Science and Processing, 2021, 127, 1.	1.1	2

#	Article	IF	CITATIONS
91	An extensive study of depth dose distribution and projectile fragmentation cross-section for shielding materials using Geant4. Applied Radiation and Isotopes, 2022, 180, 110068.	0.7	2
92	Synthesis And Optical Properties Of Nickel Doped Zinc Oxide Nanoparticles. , 2011, , .		1
93	Study of Trapping Density in Electrical Characteristics of CdTe Thin films. , 2011, , .		1
94	Structural and optical studies of CuO nanostructures. , 2014, , .		1
95	Comparative study of depth dose-distributions and partial fragmentation cross sections of 56Fe ions on polyethylene using GEANT4. Nuclear Instruments & Methods in Physics Research B, 2014, 328, 8-13.	0.6	1
96	The photocatalytic investigation of methylene blue dye with Cr doped zinc oxide nanoparticles. AIP Conference Proceedings, 2015, , .	0.3	1
97	Effect of Sr2+, Ba 2+ and Ta5+ Ions on Structural and Electrical Properties of BNKT Ceramics. Materials Today: Proceedings, 2015, 2, 2784-2788.	0.9	1
98	Quality of local scale surface weather analogs over the north-west Himalaya (NWH), India. Journal of Earth System Science, 2019, 128, 1.	0.6	1
99	Spatio-temporal variability of binary weather patterns and precipitation amounts of short time intervals during winter period over the north-west Himalaya (NWH). Journal of Earth System Science, 2019, 128, 1.	0.6	1
100	Computational study of fragmentation cross-sections for 28Si ions in various media using GEANT4. Nuclear Instruments & Methods in Physics Research B, 2020, 464, 5-11.	0.6	1
101	L-cysteine functionalized graphene quantum dots for sub-ppb detection of As (III). Nanotechnology, 2021, 33, .	1.3	1
102	Structural and optical studies of Sr and Mn doped ZnO nanoparticles. , 2013, , .		0
103	Investigation of variation of energy of laser beam on structural, electrical and optical properties of pulsed laser deposited CuO thin films. , 2014, , .		0
104	Investigation of structural, optical and photocatalytic properties of W(0.99)Pd(0.01)O3 nanoparticles. AIP Conference Proceedings, 2019, , .	0.3	0
105	The synthesis, structural, optical and electrical characterizations of double perovskite oxide Y2CuCoO5. AIP Conference Proceedings, 2020, , .	0.3	0
106	Fragmentation cross-section study of 28Si ions on 12C target with simulation toolkit GEANT4. AIP Conference Proceedings, 2020, , .	0.3	0
107	Monte Carlo simulation study for proton therapy at energy range 62â€MeV – 240â€MeV using GEANT4. AIP Conference Proceedings, 2021, , .	0.3	0
108	Quality of Local Scale Surface Weather Analogs in Two Climatologically and Geographically Distinct Mountainous Regions. Meteorology and Atmospheric Physics, 2022, 134, 1.	0.9	0